Hydrology Research

Hydrology Research Vol 55 No 9, 921 doi: 10.2166/nh.2024.052

Both meteorological droughts and human activities modulated groundwater variations in the northern Yellow River Basin

Xuening Yang [a,b], Xingmin Shao[a,c], Ning Ma[a], Xuanze Zhang[a], Jing Tian[a], Zixuan Tang[a,c], Yuyin Chen[a,c], Xiaoqiang Tian[d], Rui Feng[d], Tongjing Wu[d], Nan Bian[d], Ping Miao[e], Hongli Ma[e], Bing Chen[d] and Yongqiang Zhang [a,*]

[a] Key Laboratory of Water Cycle and Related Land Surface Processes, Institute of Geographic Sciences and Natural Resources Research, Chinese Academy of Sciences, Beijing 100101, China
[b] Sino-Danish College, University of Chinese Academy of Sciences, Beijing 100049, China
[c] University of Chinese Academy of Sciences, Beijing 100049, China
[d] Flood and Drought Disaster Prevention Technology Center, Ordos Water Conservancy Bureau, Inner Mongolia, Ordos 017000, China
[e] River and Lake Protection Center, Ordos Water Conservancy Bureau, Inner Mongolia, Ordos 017000, China
*Corresponding author. E-mail: zhangyq@igsnrr.ac.cn

XY, 0009-0001-4688-9891; YZ, 0000-0002-3562-2323

ABSTRACT

Groundwater level declines are largely associated with natural processes and human activities. In particular, the drivers of groundwater change can be more complex during meteorological drought owing to human activities. However, disentangling their specific contribution remains poorly understood. By focusing on semiarid ecosystems in the northern Yellow River Basin – the Ordos – here we elucidate the impact of human activities on the propagation of meteorological droughts to groundwater systems. To comprehensively analyze groundwater variations, we employ the K-means, categorizing them into four distinct patterns. Based on the Pearson correlation coefficient analysis between standardized precipitation index (SPI) and groundwater depth (GWD), we found that the majority of lag time for GWD response to SPI is less than 3 months, and the drivers influencing GWD are classified into three categories: SPI, human activities related to SPI, and human activities unrelated to SPI. Our results reveal that both meteorological droughts and human activities jointly influence GWD across the entire region. Notably, human activities unrelated to SPI have the greatest impact in the irrigation district of Ordos, followed by the western part of Ordos and the Mu Us sandy land in central Ordos. Our findings can guide us to formulate effective drought management policies and practices in semiarid regions.

Key words: groundwater depth, human activities, meteorological drought, propagation characteristics, Yellow River Basin

HIGHLIGHTS

- Groundwater variability in the Ordos, northern Yellow River Basin shows four major patterns.
- The variation of groundwater depth mostly is less than 3-month lag behind the variation of SPI.
- The GWD is mainly influenced by meteorological factors at 60% monitoring wells, but by human activities at the rest.

GRAPHICAL ABSTRACT

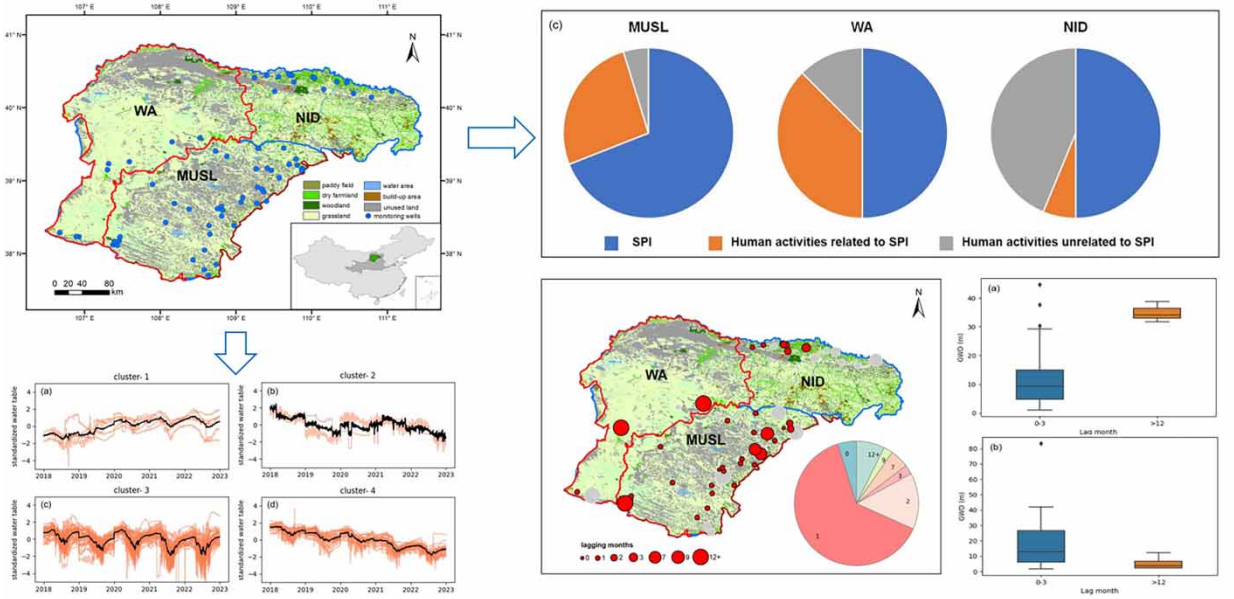

The groundwater variations are categorized into four distinct patterns with K-means.

Based on the Pearson Correlation Coefficient analysis between Standardized Precipitation Index (SPI) and groundwater depth (GWD), the factors influencing GWD, and the lag time for GWD response to SPI are identified.

1. INTRODUCTION

Groundwater is a critical source of freshwater (Zhang *et al.* 2019; Scanlon *et al.* 2023), providing approximately half of the water used for global irrigation and the majority of the drinking water for domestic needs (Jasechko & Perrone 2021; Noori *et al.* 2023). With population growth and increased water demand, groundwater withdrawal has increased eightfold to meet human needs (Hanasaki *et al.* 2018; Wada *et al.* 2014; Bierkens & Wada 2019). Simultaneously, the expansion of irrigated agriculture has intensified groundwater withdrawal, particularly in semiarid regions where groundwater may be the only reliable source of water due to the absence of permanent surface water (Wada *et al.* 2012; Ashraf *et al.* 2021). Frappart & Ramillien (2018) found that global groundwater storage has been declining at an increasing rate of depletion. Continuous decreases in groundwater levels can lead to serious issues, such as land subsidence, seawater intrusion, and a decline in agricultural and industrial productivity (Lin *et al.* 2022). Therefore, it is crucial to understand the influential factors contributing to the groundwater decline.

Increases in drought frequency, duration, and intensity have greatly exacerbated groundwater depletion (Zhao *et al.* 2022). Given the prevalence of frequent drought events, examining how groundwater depth (GWD) may change in response to meteorological droughts is crucial. Meteorological droughts exert both direct and indirect impacts on groundwater systems (Thomas *et al.* 2017). Direct impacts involve climate variables, such as precipitation, influencing groundwater recharge and causing fluctuations in groundwater levels (Kubicz *et al.* 2019). Indirect impacts encompass certain human activities aimed at alleviating droughts (Shah *et al.* 2021), which intensify the consumption of groundwater induced by meteorological droughts (Schober *et al.* 2018; Yang *et al.* 2020). Ojha *et al.* (2018) found that severe droughts resulted in approximately a 2% loss of total aquifer system storage in California's Central Valley. Agarwal *et al.* (2023) discovered that the rate of groundwater water storage depletion is faster during the drought periods in Central Valley. Long *et al.* (2013) observed a significant depletion of water storage, monitored with the GRACE satellite, induced by the 2011 drought in Texas. Previous studies have revealed the influence of droughts on groundwater, elucidating that the process of propagation from meteorological droughts to groundwater is also crucial.

Numerous studies have focused on the propagation of meteorological droughts to groundwater in natural states or monitoring wells without human elements (Mishra *et al.* 2018; Aadhar & Mishra 2020). These studies reveal the mechanism by which natural elements, such as soil moisture (Zhang *et al.* 2021a), aquifer characteristics (Bloomfield & Marchant 2013),

and vegetation (Liu *et al.* 2023), influence the propagation of meteorological droughts to groundwater systems (Apurv *et al.* 2017). Furthermore, these studies contribute to a deeper understanding of how meteorological droughts influence groundwater systems. However, human activities complicate the propagation from meteorological droughts to groundwater systems, and this complexity may exhibit spatial heterogeneity (Zhang *et al.* 2022b, 2022c). For instance, Yang *et al.* (2020) found that human activities reduce the severity of hydrological droughts in the south of China but exacerbate hydrological droughts in the north. While some studies have revealed the intervention of human activities in the influence of meteorological droughts on streamflow (Tijdeman *et al.* 2018; Zhang *et al.* 2022b), research on how the human activities intervene in the propagation from meteorological droughts to groundwater systems is rare. Given the significant role of groundwater in water resources and the increasing frequency of drought events due to climate change, it is crucial to uncover the mechanisms by which meteorological droughts propagate to groundwater systems in regions with high levels of human activities.

The Ordos, located in the northern Yellow River Basin, is ecologically fragile and frequently disturbed by human activities (Ma *et al.* 2019). Serving as an essential ecological barrier in northern China, Ordos has witnessed the implementation of various ecological restoration projections, including the Natural Forest Conservation Program (NFCP) and the Grain for Green Program (GFGP) (Feng *et al.* 2016; Chen *et al.* 2019). The Mu Us sandy land (MUSL) within Ordos stands as one of the most successful examples of ecological restoration and desertification reversal (Tian *et al.* 2015; Zhang & Huisingh 2018). Numerous studies confirm the increasing vegetation coverage in MUSL (Zhang & Wu 2020; Zhao *et al.* 2020; Sun *et al.* 2021), and this vegetation restoration has led to heightened groundwater consumption (Zhang & Wu 2020; Luan *et al.* 2023). In addition, farmlands, primarily distributed in the north, rely heavily on groundwater irrigation. Some studies indicate that groundwater can buffer the impact of drought events on vegetation (Deng *et al.* 2022) and delay the propagation from meteorological droughts to agricultural droughts (Fawen *et al.* 2023).

However, it remains unknown whether the impact of meteorological droughts on groundwater will change under the influence of human activities, particularly in the semiarid regions with fragile ecosystems. As such, major objectives of this study are (1) to identify the spatiotemporal variation characteristics of groundwater levels in Ordos; (2) to reveal the intervention of human activities in the propagation from meteorological droughts to groundwater systems; and (3) to clarify the lag time of groundwater system's response to meteorological droughts. The grand aim is to support the local government's efforts to manage human activities, thus implementing measures to cope with droughts.

2. MATERIALS AND METHODS

2.1. Study region

The Ordos is located in the northern Yellow River Basin in Northwest China (106°42′40″–111°27′20″E, 37°35′24″–40°51′40″N) (Figure 1). It features a typical semiarid climate characterized by scarce precipitation and high potential evapotranspiration (PET). Precipitation in the region ranges from 192 to 400 mm, decreasing from east to west (Guo *et al.* 2017). Due to this semiarid climate, groundwater serves as the primary source for drinking, irrigation, and chemical industries (Guangcai *et al.* 2008). Statistical results indicate that approximately 64% of water consumption in Ordos is derived from groundwater (Yin *et al.* 2012). The heavy reliance on groundwater has led to a significant decline in the groundwater table in Ordos since the 1990s (Jiang *et al.* 2018; Zhang *et al.* 2021b). The main aquifer in Ordos is the thick Cretaceous sandstone with sporadic clay lenses, constituting an unconfined aquifer with a maximum thickness of around 1,000 m (Guangcai *et al.* 2008; Jiang *et al.* 2018). This aquifer is covered by a thin layer of sand (Xie *et al.* 2021). Based on geographic features, the Ordos is divided into three subregions: the north irrigation district (NID), the MUSL, and the west area (WA). These subregions and their boundaries are shown in Figure 1.

2.2. Data

We used the standardized precipitation index (SPI) (McKee *et al.* 1993; Xu *et al.* 2015; Eini *et al.* 2023) to represent the meteorological drought, which could be derived from precipitation (see Section 2.3). Here, the monthly precipitation data from 1970 to 2020 were obtained from the National Tibetan Plateau Data Center Third Pole Environment Data Center (https://data.tpdc.ac.cn/zh-hans/data/faae7605-a0f2-4d18-b28f-5cee413766a2) at a spatial resolution of 1 km (Shouzhang 2020). The daily GWD data for 67 monitoring wells in the Ordos, covering the period from 2018 to 2022, were sourced from the local hydrology departments. We used the daily GWD data to cluster the variation of the groundwater dynamics.

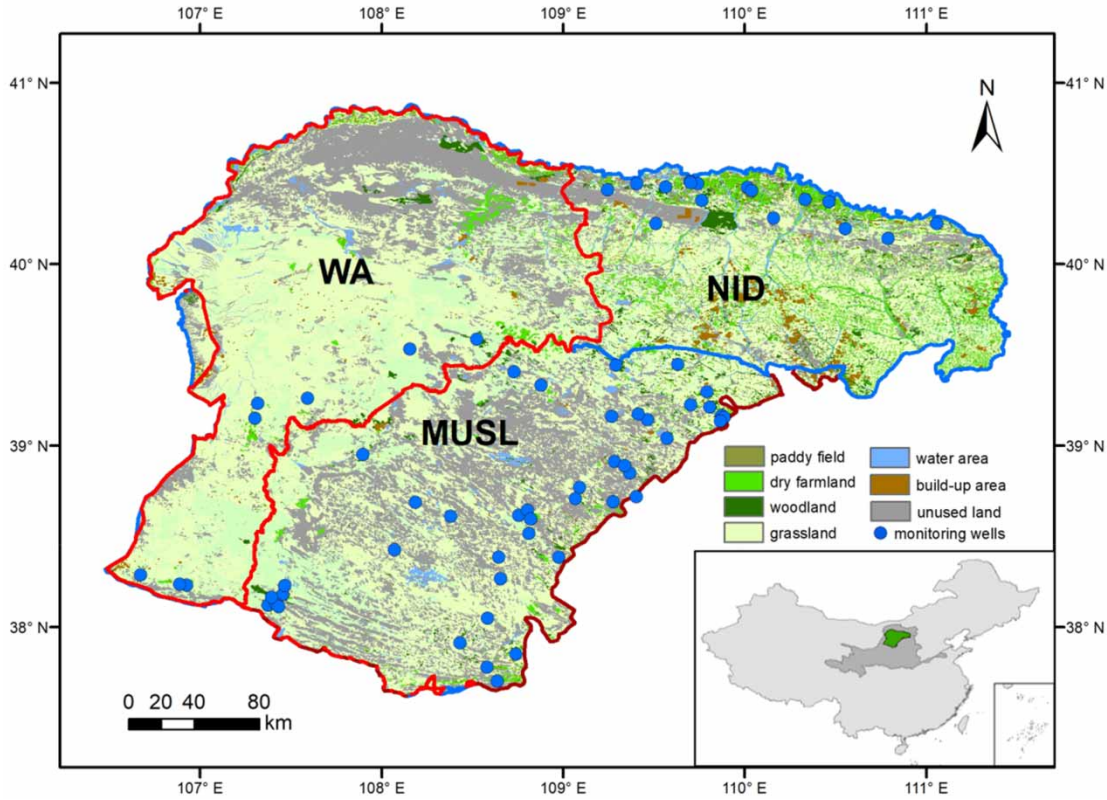

Figure 1 | The geographical location and underlying surface of Ordos. NID, the north irrigation district; WA, the west area; MUSL, the Mu Us sandy land.

We aggregated the daily GWD data into a monthly scale by averaging them for a better examination of its correlation with SPI.

2.3. Calculation of the SPI

Precipitation deficit is a key characteristic of meteorological droughts, and precipitation exhibits spatial discrepancies across different regions. When characterizing drought solely based on precipitation, the comparability of space and time becomes insufficient, thereby limiting the spatial and temporal scales of studies. Therefore, the SPI was used for monitoring meteorological drought in semiarid regions, which is recommended by the World Meteorological Organization (McKee *et al.* 1993; Hayes *et al.* 2011). The SPI, calculated with input from precipitation data, can be calculated at various time scales, offering substantial flexibility across different time intervals (Vicente-Serrano *et al.* 2010). Its standardization empowers the SPI to evaluate precipitation deficit status in diverse regions, demonstrating robust spatial expansibility (Guttman 1998; Vicente-Serrano *et al.* 2010). The details of the SPI calculation are as follows:

(1) Suppose the precipitation during a period is x, the probability density function following Γ distribution is as follows:

$$f(x) = \frac{1}{\beta^{\gamma}\Gamma(\gamma)} x^{\gamma-1} e^{-x/\beta} \tag{1}$$

where x is the amount of precipitation over consecutive months and β and γ are the scale and shape of the distribution, which are calculated using the maximum likelihood estimation.

$$\hat{\gamma} = \frac{1 + \sqrt{1 + 4A/3}}{4A} \tag{2}$$

$$\hat{\beta} = \frac{\bar{x}}{\hat{\gamma}} \tag{3}$$

$$A = \ln \bar{x} - \frac{1}{n}\sum_{i=1}^{n} \ln x_i \tag{4}$$

where x_i is the ith value in the precipitation series and $\bar{x}$ is the average precipitation. The function $\Gamma(\gamma)$ is the gamma function given as

$$\Gamma(\gamma) = \int_0^{\infty} y^{\alpha-1} e^{-y} dy \tag{5}$$

After the probability density parameters are estimated, the cumulative probability of precipitation can be expressed as

$$F(x) = \frac{1}{\beta^{\gamma}\Gamma(\gamma)} \int_0^{x} x^{\gamma-1} e^{-x/\beta} dx \tag{6}$$

$$\mathrm{SPI} = S \frac{t - (c_2 t + c_1)t + c_0}{((d_3 t + d_2)t + d_1)t + 1} \tag{7}$$

where $t = \sqrt{\ln \frac{1}{H(x)^2}}$ and $F(x)$ is the probability distribution of precipitation. When $F(x) > 0.5$, $S = 1$ and $H(x) = 1 - G(x)$, and when $F \leq 0.5$, $S = -1$ and $H(x) = G(x)$. The variables in Equation (7) are generally taken as $c_0 = 2.515517$, $c_1 = 0.802853$, $c_2 = 1.432788$, $d_1 = 1.432788$, $d_2 = 0.189626$, and $d_3 = 0.001308$ (Lloyd-Hughes & Saunders 2002; Asadi Zarch *et al.* 2015; Xu *et al.* 2015; Huang *et al.* 2017; Tian 2022).

Considering the cumulative effect of meteorological droughts, we calculated the SPI at time scales varying from 1 to 48 months.

2.4. Classified characteristics of groundwater interannual variations

We employed a two-step approach for the GWD clustering. The first step is to realign the GWD time series and measure the similarity among groundwater time series. In the first step, we used the dynamic time warping (DTW) algorithm. DTW can find optimal global alignment between sequences (Petitjean *et al.* 2011) and is widely used to quantify the similarity between sequences (Kruskall & Liberman 1983; Aach & Church 2001; Bar-Joseph *et al.* 2002; Gilleland & Roux 2015; Mantas *et al.* 2015). In this method, each point of the first sequence is compared with any point of the second sequence. Finally, sequences with similar patterns that occurred in different periods are considered similar (Izakian *et al.* 2015). In the second step, we used the K-means algorithm to cluster rescaled time series. K-means is one of the most widely used algorithms for clustering (Fejes Tóth 1959; Ball & Hall 1965; MacQueen 1967; Lloyd 1982), because of its simplicity, efficiency, and empirical success (Jain 2010). In this study, we wrote a program in the Python language and performed the two successive steps: DTW algorithm and K-means clustering.

2.5. Identifying the major contributors to changes in GWD

The Pearson correlation coefficient (PCC) is used to reflect the strength of relationships between SPI and GWD. For two variables X and Y (which are SPI and GWD in this study), PCC can be expressed as

$$\mathrm{PCC} = \frac{E(XY) - E(X)E(Y)}{\sqrt{\sigma^2(X)}\sqrt{\sigma^2(Y)}} \tag{8}$$

where $E(X)$, $E(Y)$, and $E(XY)$ are the expectations and $\sigma^2(X)$ and $\sigma^2(Y)$ are the variances.

In this study, we calculated the PCC between GWD and SPI at time scales ranging from 1 to 48 months to identify the time scale of SPI with the most significant impact on GWD. If the SPI has impacts on GWD, the PCC between SPI and GWD is

negative. The time scale of SPI with the minimum PCC is considered to have the greatest impact on GWD. We categorize drivers based on the absolute value of the PCC and the *p*-value into three categories. When $|PCC| > 0.5$ and $p < 0.05$, SPI has a strong and significant impact on GWD, and the primary driver influencing the GWD is SPI alone. When $|PCC| < 0.5$ and $p < 0.05$, SPI has a weak but significant impact on GWD, with its influence disturbed by human activities related to meteorological droughts, such as irrigation and ecological restoration (Udovičić *et al.* 2007; Feng *et al.* 2020). When $p > 0.05$, the impact of SPI on GWD is insignificant, and the primary drivers influencing GWD are human activities unrelated to meteorological droughts, such as managed groundwater recharge projects.

2.6. Calculation of lag time

Typically, the variation in GWD lags behind the variation in SPI. To determine the lag time, we calculated the PCC between GWD and SPI for the preceding 1–48 months. Similarly, the month with the minimum PCC between GWD and SPI is considered the lag time for GWD's response to meteorological droughts, which has been widely used in drought propagation studies (Zhang & Jia 2013; Wang *et al.* 2017; Wan *et al.* 2023).

3. RESULTS

3.1. Variation of groundwater table

The variations in groundwater table observations in Ordos are categorized into four patterns, as illustrated in Figure 2. For the first pattern, the groundwater table consistently increases over time (Figure 2(a)). The second pattern is a zigzag pattern in the fluctuation of the groundwater table, with an overall declining trend, suggesting frequent and excessive water extraction (Figure 2(b)). The third one shows seasonal fluctuations in the groundwater table, decreasing in summer and increasing in winter, maintaining a relatively flat interannual scale (Figure 2(c)). This pattern indicates a balance between groundwater recharge and discharge, possibly influenced by precipitation or moderate seasonal human activities. Figure 2(d) displays that in the fourth pattern, the groundwater table also fluctuates seasonally, but with overall decreasing trends. This pattern could be due to excessive seasonal water extraction, such as in the case of excessive irrigation.

The spatial distribution of all monitoring wells clustered to the four patterns is also shown in Figure 2(e). Initially, we hypothesized that the variation in the groundwater table might be influenced by land use classification, and the monitoring wells in each category would follow distinct spatial rules. However, the spatial distribution rules for each category are not evident. This means the land use classification is not the direct factor influencing the groundwater dynamics. Since meteorological factors and human activities are common factors influencing groundwater dynamics, we further use statistical methods to explore the driving factors of groundwater dynamics.

3.2. Correlation between GWD and SPI

Correlation analysis is employed to identify the drivers influencing GWD in each monitoring well. Figure 3(a) illustrates the results of the correlation analysis between GWD and SPI. The range of PCC values for Ordos is −0.072 to −0.826, where the MUSL and WA have most of the monitoring wells with strong negative correlations (−0.212 to −0.822) while the NID has a higher proportion of SPI-unrelated wells. Following the classification criteria mentioned in Section 2.5 and considering the PCC values, the identified drivers include SPI, human activities related to SPI, and human activities unrelated to SPI. The spatial distribution of each driver influencing GWD is depicted in Figure 3(b). The majority of the monitoring wells in Ordos are dominated by SPI, while some monitoring wells, primarily in the NID, are strongly influenced by human activities unrelated to SPI. Figure 3(c) presents the statistical results of drivers influencing GWD. In the MUSL, 69.05% of monitoring wells are influenced by SPI, 26.19% by human activities related to SPI, and 4.76% by human activities unrelated to SPI. In the WA, 50% of monitoring wells are influenced by SPI, 37.5% by human activities related to SPI, and 12.5% by human activities unrelated to SPI. In the NID, half the monitoring wells are influenced by SPI and 43.75% are influenced by human activities unrelated to SPI. Overall, human activities unrelated to SPI have the greatest impact on the NID, followed by the WA and the MUSL.

3.3. Lag time of GWD in response to SPI

The lag time of the GWD response to SPI is depicted in Figure 4. In 4.88% of monitoring wells, the GWD responds to SPI at the current month, and in 63.41% of monitoring wells, the lag time of the GWD response to SPI is 1 month, while 14.63% of monitoring wells exhibit a lag time of 2 months. In the remaining monitoring wells, the lag times of GWD response to SPI are

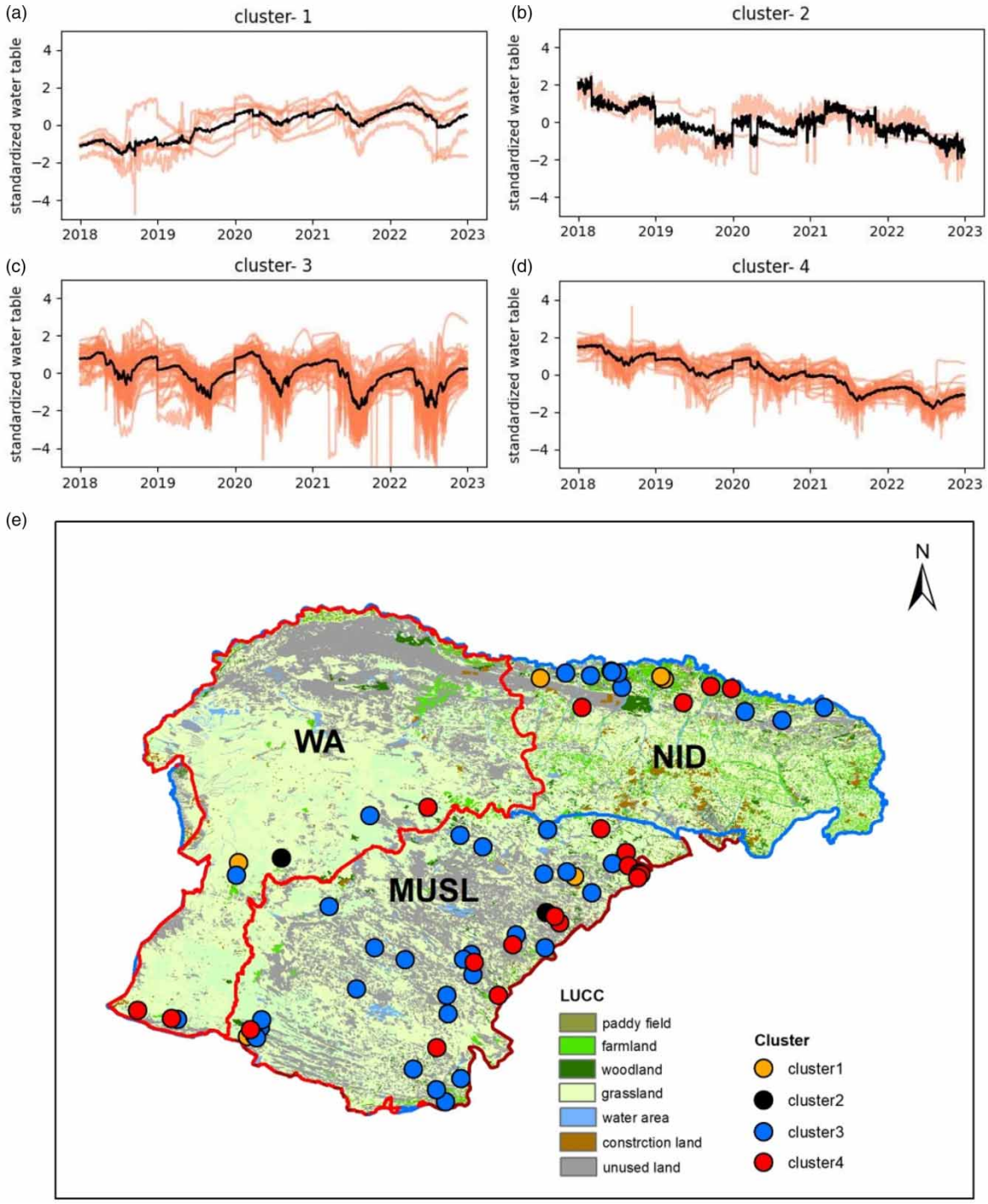

Figure 2 | The variation of groundwater table from 2018 to 2022 in Ordos. (a–d) Four patterns of the variation of the groundwater table. The vertical axis represents the standardized water stable. (e) The spatial distribution of each category of groundwater table.

3, 7, 9, and even more than 12 months in three monitoring wells. Figure 5 depicts the relationship between GWD and lag times. As shown in Figure 5(a), in the monitoring wells influenced by SPI, GWD at a lag of more than 12 months exceeds that at a lag of 0–3 months in response to SPI. In Figure 5(b), for monitoring wells impacted by human activities, GWD with a lag response to SPI of 0–3 months is slightly greater than that with a lag time of more than 12 months in response

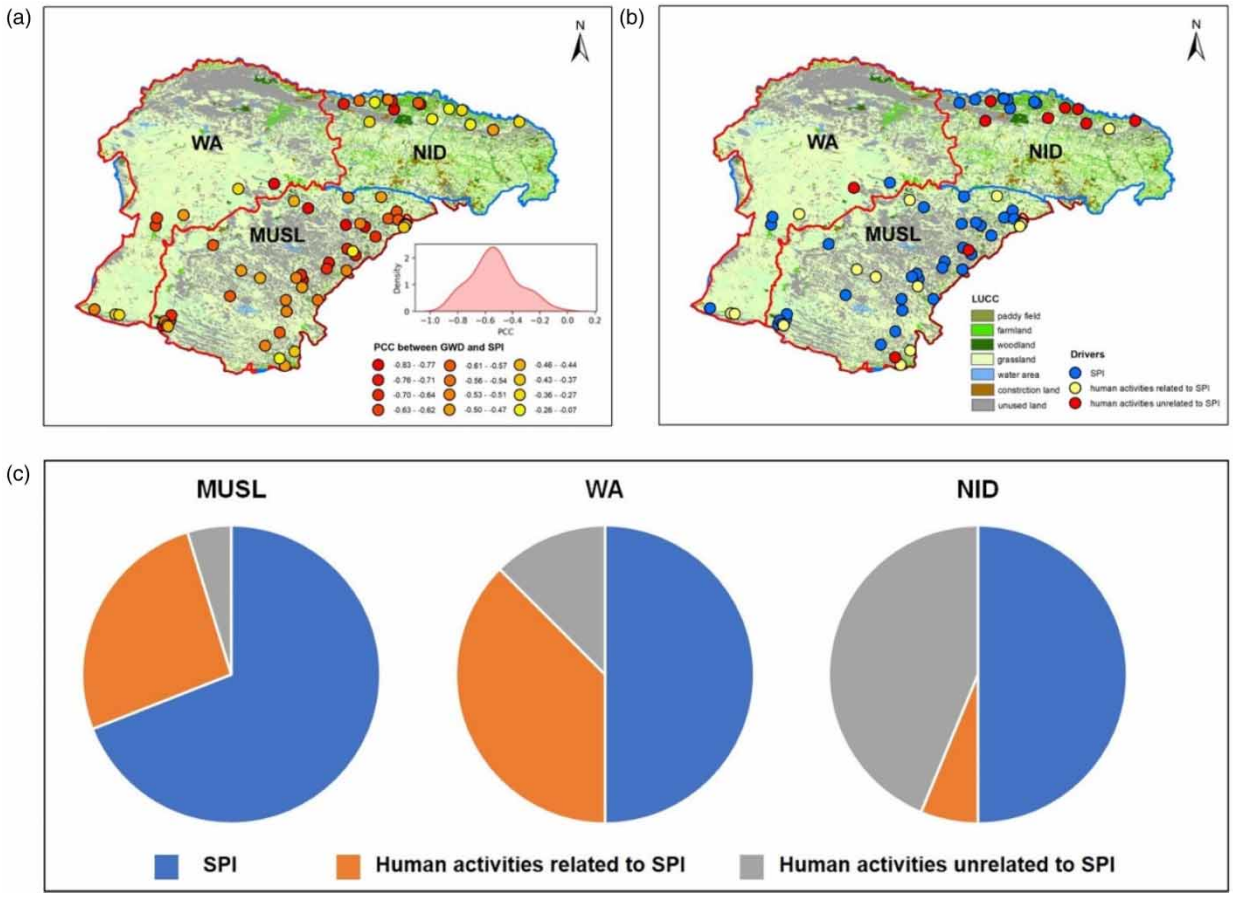

Figure 3 | Correlation analysis between GWD and SPI. (a) PCC between GWD and SPI of each monitoring well. (b) The spatial distribution of drivers influences the variation of GWD. (c) The percentage of each driver in MUSL, WA, and NID.

to SPI. Therefore, under natural conditions, deep groundwater levels can delay its response to meteorological droughts, and human activities disrupt the propagation from meteorological droughts to GWD.

4. DISCUSSION

4.1. Four patterns of groundwater dynamics in Ordos

The groundwater dynamics are divided into four patterns in Ordos. The first pattern is continuously increasing. This may be caused by irrigation-driven deep percolation (Huo *et al.* 2011). It can also be attributed to the geological structure. For instance, Guangcai *et al.* (2008) found that the NID belongs to the Cretaceous Aquifer System, where precipitation is the major recharge source and groundwater flow is controlled by topography. Due to the higher topography than surrounding areas, there may be no lateral recharge from the surrounding groundwater systems. Chen *et al.* (2024) found a similar increasing pattern in southeastern Australia during the millennial drought period and believe that the increasing trends may be related to lateral recharge from mountainous areas. The second pattern is jagged decreasing, which may be caused by frequent anthropogenic abstraction for industry. The third and fourth patterns are both seasonal fluctuations, while the third one is annually flat and the fourth one decreases annually. The crop growth season in Ordos is from May to October. According to Figure 2(c) and 2(d), the groundwater table decreases during the crop growth season and then increases after harvesting. Therefore, we infer that the third and fourth patterns are caused by irrigation extraction (Ju *et al.* 2012). If the extraction is similar in magnitude to the recharge, the annual groundwater table is relatively stable and belongs to the third pattern. If the groundwater abstraction is larger than the recharge, the water table decreases annually, belonging to the fourth pattern.

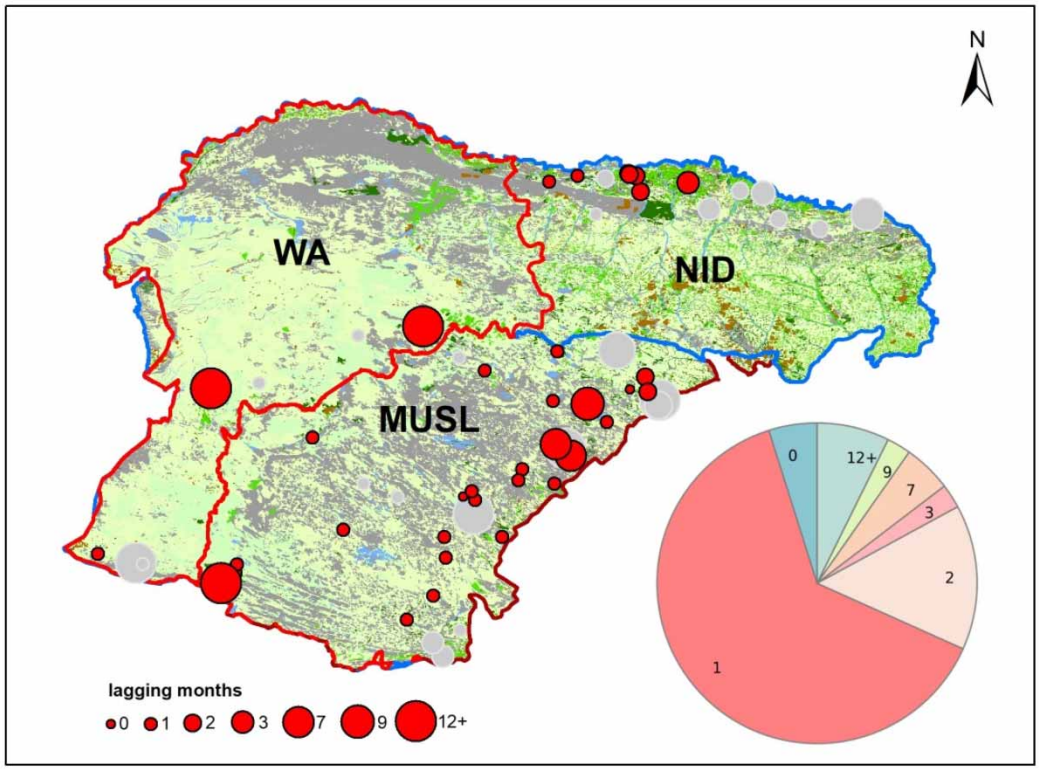

Figure 4 | The lag time of GWD response to SPI in each monitoring well. The pie graph shows the percentage of monitoring wells with different lag times. The red points represent the monitoring wells influenced by SPI, and the gray points represent the monitoring wells disturbed by human activities.

4.2. Interactions between meteorological droughts, human activities, and groundwater dynamics

Groundwater recharge occurs through precipitation and various human activities, such as irrigation recharging (Jasechko *et al*. 2014; Qi *et al*. 2023), while discharge is facilitated by evapotranspiration and pumping (Doble *et al*. 2006). In semiarid regions, precipitation plays a crucial role in the variability of GWD (Luan *et al*. 2023). To elucidate the impacts of meteorological droughts on GWD, we calculated the SPI as the meteorological drought indicator and analyzed the correlation relationship between SPI and GWD. The strong and significant correlations between SPI and GWD in more than 60% of

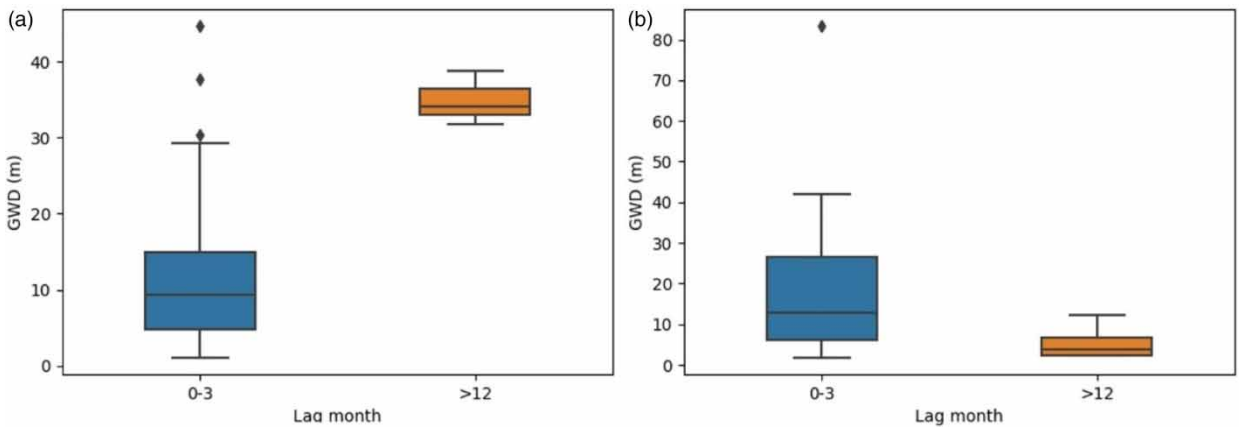

Figure 5 | The relationship between lag time and GWD in the monitoring wells influenced by SPI (a) and human activities (b).

monitoring wells in Ordos suggest that the variability of GWD is primarily influenced by meteorological conditions. Less precipitation affects groundwater resources by decreasing soil water infiltration (Han *et al*. 2021).

A weak but still significant correlation in some monitoring wells indicates that human activities disturb the propagation from meteorological droughts to GWD, particularly activities related to meteorological droughts, such as irrigation in NID and ecological restoration in MUSL. In the dry season, deficit precipitation increases water demand, leading to more groundwater extraction to alleviate water stress for crops, consequently lowering the groundwater table (Zhang *et al*. 2021a). However, in wet seasons, sufficient irrigation may not raise the groundwater table due to reduced water availability for recharge (Zomlot *et al*. 2015; Lorenzo-Lacruz *et al*. 2017). In ecology, densely populated artificial revegetation increases groundwater extraction and may intensify the groundwater drought in the dry season (Lu *et al*. 2018; Han *et al*. 2020) because vegetation roots extract more groundwater for transpiration, especially in dry years (Wu *et al*. 2016). Some studies demonstrate that revegetation can improve soil conditions and enhance infiltration, but groundwater is not recharged due to the transpiration with additional soil moisture in semiarid regions (Bartley *et al*. 2006; Teuling *et al*. 2013; Gao *et al*. 2015). In general, vegetation responds to water stress by partially closing the stomata to reduce transpiration, which limits the carbon uptake by photosynthesis (Peters *et al*. 2018). Over places with deficit and deep groundwater, drought results in the reduction of gross primary production (Zhang *et al*. 2022a). Shallow and sufficient groundwater can maintain the stomatal conductance opening and buffer the effects of drought on vegetation (Meinzer *et al*. 2016; Deng *et al*. 2022). Therefore, overexploitation of groundwater for irrigation or over-revegetation will decrease groundwater availability, which aggravates the response of vegetation and agriculture to drought (Wu *et al*. 2017). In addition, water in reservoirs can continuously recharge groundwater, disrupting the propagation from meteorological droughts to groundwater systems (Apurv *et al*. 2017).

There is still a part of monitoring wells where GWD has an insignificant correlation relationship with SPI, likely due to human activities unrelated to meteorological droughts, such as managed aquifer recharge projects. In the pursuit of sustainable development in Ordos, the local government artificially replenishes groundwater to strike a balance between exploitation and replenishment. Coal mining is also an anthropometric intervention for groundwater dynamics. Ordos is rich in coal resources, and Xie *et al*. (2018) found that large-scale mining may damage the stratum structure of the mining area and lead to groundwater loss. The lack of correlation between meteorological droughts and groundwater tables is also observed in some studies. For instance, Lorenzo-Lacruz *et al*. (2017) found that tourism pressure exacerbates groundwater exploitation during summer, leading to an insignificant correlation relationship between SPI and the standardized groundwater index. Wendt *et al*. (2021) found that managed aquifer recharge significantly reduced groundwater in both duration and magnitude. Another possible reason for the insignificant impacts of meteorological droughts on GWD may be the continuous overuse of groundwater (Wendt *et al*. 2021), where groundwater abstraction surpasses precipitation recharge, resulting in an increase in precipitation but a decline in the groundwater table. The intervention of human activities in groundwater is various. Irrigation and revegetation reduce the groundwater, coal mining changes the geological structure, and reservoirs and managed aquifer recharge projects change the natural process of groundwater recharge. These human activities complicate the groundwater dynamics, which enhances the difficulty of water resource prediction and management.

4.3. Lag time analysis of SPI and GWD

The lag time represents the speed of propagation of meteorological drought to groundwater systems (Schuler *et al*. 2022). The length of lag time that GWD responds to SPI is related to the depth of groundwater level. Throughout the region, the average GWD with a lag time of 0–3 months is much smaller than the average GWD with a lag time larger than 12 months because the surface water needs more time to recharge groundwater when the groundwater table is deeper (Schreiner-McGraw & Ajami 2021). Some monitoring wells exhibit abnormal GWD with a lag time of 0–3 months, closely resembling the average GWD with a lag time larger than 12 months. This abnormality may be caused by human activities related to meteorological droughts, such as irrigation. During meteorological droughts, farmers tend to extract more groundwater to alleviate water stress on crops. During such times, the GWD has no impact on the lag time of GWD responding to meteorological droughts. Similarly, ecological restoration in semiarid regions may also intervene in the influence of GWD on the lag time. In general, vegetation species used for ecological restoration are drought-tolerant, with well-developed root systems (Liu *et al*. 2021). The drier climate can trigger plants to extend their roots to abstract deeper groundwater and reduce water stress (Liu *et al*. 2021). Consequently, the lag time of GWD to meteorological droughts may be shortened.

4.4. Indicators for meteorological droughts

Both SPI and the standardized precipitation evapotranspiration index (SPEI) serve as crucial indicators for meteorological droughts (McKee *et al*. 1993; Vicente-Serrano *et al*. 2010; Yao *et al*. 2018). Given the relatively small size of Ordos, it necessitates data with fine spatial resolution. The calculation of SPEI relies on the key variable of PET (Vicente-Serrano *et al*. 2010). There are three common equations for calculating PET, namely, the Penman–Monteith equation, the Thornthwaite equation (Thornthwaite 1948), and the Hargreaves equation (Hargreaves & Samani 1985). Among these, Thornthwaite and Hargreaves methods focus solely on temperature, while the Penman–Monteith equation considers multiple meteorological factors influencing PET, including wind speed, relative humidity, radiation, and air pressure (Adnan *et al*. 2021; Cao *et al*. 2022). Due to the lack of high-precision products of wind speed and relative humidity, the Penman–Monteith equation is not adopted in this study. Some studies have challenged the conventional belief that temperature is the primary meteorological driver influencing PET in semiarid regions. For instance, Liu *et al*. (2024) found that relative humidity is the most sensitive factor for PET in semiarid regions. Yin *et al*. (2021) found that the PET in the Chinese northwest arid regions is more sensitive to radiation, wind speed, and relative humidity than average temperature during the growth season. Therefore, relying solely on temperature for calculating PET could introduce uncertainties. These uncertainties may further accumulate into SPEI, potentially impacting the final analysis.

5. CONCLUSIONS

This study explores the variation of GWD in Ordos, the northern Yellow River Basin, and distinguishes the impacts of meteorological droughts and human activities on the GWD. There are four patterns of groundwater dynamics in Ordos, including continuous increased pattern, jagged declined pattern, fluctuated seasonally but annual stable pattern, and fluctuated seasonally but declined overall. We found that the GWD in Ordos is influenced by both meteorological droughts and human activities, and the GWD is influenced by meteorological factors at the majority of monitoring wells. The lag time of GWD response to meteorological droughts is related to the absolute magnitude of GWD, and most of the lag times are less than 3 months. Our results are helpful for local governments to manage human activities and implement measures to cope with droughts. For instance, predicting meteorological factors accurately at seasonal to annual scales can increase the prediction skill for groundwater dynamics and prepare drought mitigations in advance. Furthermore, promoting water-saving irrigated agriculture and revegetating moderately is a practical way to avoid overexploitation of groundwater. Nevertheless, our study is limited by data availability, making quantification of human activities challenging. Furthermore, GWD may be influenced by multiple human activities, and how to isolate the impact of each human activity on GWD deserves future exploration.

ACKNOWLEDGEMENTS

This study was financially supported by the Inner Mongolia Autonomous Region Water Conservancy Research Special Project (Grant No. NSK202301), the Ordos Major Science and Technology Projects (Grant No. ZD20232302), and the National Natural Science Foundation of China (Grant No. 42361144709). We appreciate the valuable contributions of anonymous reviewers, whose constructive and critical comments and suggestions greatly improved the paper's quality.

DATA AVAILABILITY STATEMENT

All relevant data are included in the paper or its Supplementary Information.

CONFLICT OF INTEREST

The authors declare there is no conflict.

REFERENCES

Aach, J. & Church, G. M. 2001 Aligning gene expression time series with time warping algorithms. *Bioinformatics* **17** (6), 495–508.

Aadhar, S. & Mishra, V. 2020 On the projected decline in droughts over South Asia in CMIP6 multimodel ensemble. *Journal of Geophysical Research: Atmospheres* **125** (20), e2020JD033587.

Adnan, R. M., Mostafa, R. R., Islam, A. R. M. T., Kisi, O., Kuriqi, A. & Heddam, S. 2021 Estimating reference evapotranspiration using hybrid adaptive fuzzy inferencing coupled with heuristic algorithms. *Computers and Electronics in Agriculture* **191**, 106541.

Agarwal, V., Akyilmaz, O., Shum, C. K., Feng, W., Yang, T. Y., Forootan, E., Syed, T. H., Haritashya, U. K. & Uz, M. 2023 Machine learning based downscaling of GRACE-estimated groundwater in Central Valley, California. *Science of The Total Environment* **865**, 161138.

Apurv, T., Sivapalan, M. & Cai, X. 2017 Understanding the role of climate characteristics in drought propagation. *Water Resources Research* **53** (11), 9304–9329.

Asadi Zarch, M. A., Sivakumar, B. & Sharma, A. 2015 Droughts in a warming climate: A global assessment of standardized precipitation index (SPI) and reconnaissance drought index (RDI). *Journal of Hydrology* **526**, 183–195.

Ashraf, S., Nazemi, A. & AghaKouchak, A. 2021 Anthropogenic drought dominates groundwater depletion in Iran. *Scientific Reports* **11** (1), 9135.

Ball, G. H. & Hall, D. J. 1965 *Isodata, A Novel Method of Data Analysis and Pattern Classification*. Technical Report. Stanford Research Institute, Menlo Park.

Bar-Joseph, Z., Gerber, G., Gifford, D. K., Jaakkola, T. S. & Simon, I. 2002 *A New Approach to Analyzing Gene Expression Time Series Data*. Association for Computing Machinery, Washington, DC, pp. 39–48.

Bartley, R., Roth, C. H., Ludwig, J., McJannet, D., Liedloff, A., Corfield, J., Hawdon, A. & Abbott, B. 2006 Runoff and erosion from Australia's tropical semi-arid rangelands: Influence of ground cover for differing space and time scales. *Hydrological Processes* **20** (15), 3317–3333.

Bierkens, M. F. P. & Wada, Y. 2019 Non-renewable groundwater use and groundwater depletion: A review. *Environmental Research Letters* **14** (6), 063002.

Bloomfield, J. P. & Marchant, B. P. 2013 Analysis of groundwater drought building on the standardised precipitation index approach. *Hydrology and Earth System Sciences* **17** (12), 4769–4787.

Cao, S., Zhang, L., He, Y., Zhang, Y., Chen, Y., Yao, S., Yang, W. & Sun, Q. 2022 Effects and contributions of meteorological drought on agricultural drought under different climatic zones and vegetation types in Northwest China. *Science of The Total Environment* **821**, 153270.

Chen, C., Park, T., Wang, X., Piao, S., Xu, B., Chaturvedi, R. K., Fuchs, R., Brovkin, V., Ciais, P., Fensholt, R., Tommervik, H., Bala, G., Zhu, Z., Nemani, R. R. & Myneni, R. B. 2019 China and India lead in greening of the world through land-use management. *Nature Sustainability* **2**, 122–129.

Chen, Y., Zhang, Y., Tian, J., Nourani, V., Ma, N., Zhang, X., Xu, Z., Huang, Q., Tang, Z., Wei, H. & Yang, X. 2024 Groundwater exhibits spatially opposing trends during the Australian Millennium Drought. *Environmental Research Letters* **19**, 7.

Deng, W., Chen, M., Zhao, Y., Yan, L., Wang, Y. & Zhou, F. 2022 The role of groundwater depth in semiarid grassland restoration to increase the resilience to drought events: A lesson from Horqin Grassland, China. *Ecological Indicators* **141**, 109122.

Doble, R., Simmons, C., Jolly, I. & Walker, G. 2006 Spatial relationships between vegetation cover and irrigation-induced groundwater discharge on a semi-arid floodplain, Australia. *Journal of Hydrology* **329** (1–2), 75–97.

Eini, M. R., Rahmati Ziveh, A., Salmani, H., Mujahid, S., Ghezelayagh, P. & Piniewski, M. 2023 Detecting drought events over a region in Central Europe using a regional and two satellite-based precipitation datasets. *Agricultural and Forest Meteorology* **342**, 109733.

Fawen, L., Manjing, Z., Yong, Z. & Rengui, J. 2023 Influence of irrigation and groundwater on the propagation of meteorological drought to agricultural drought. *Agricultural Water Management* **277**, 108099.

Fejes Tóth, L. 1959 Sur la représentation d'une population infinie par un nombre fini d'éléments. *Acta Mathematica Academiae Scientiarum Hungarica* **10** (3), 299–304.

Feng, X., Fu, B., Piao, S., Wang, S., Ciais, P., Zeng, Z., Lü, Y., Zeng, Y., Li, Y., Jiang, X. & Wu, B. 2016 Revegetation in China's Loess Plateau is approaching sustainable water resource limits. *Nature Climate Change* **6** (11), 1019–1022.

Feng, P., Wang, B., Luo, J.-J., Liu, D. L., Waters, C., Ji, F., Ruan, H., Xiao, D., Shi, L. & Yu, Q. 2020 Using large-scale climate drivers to forecast meteorological drought condition in growing season across the Australian Wheatbelt. *Science of The Total Environment* **724**, 138162.

Frappart, F. & Ramillien, G. 2018 Monitoring groundwater storage changes using the gravity recovery and climate experiment (GRACE) satellite mission: A review. *Remote Sensing* **10** (6), 829.

Gao, Z., Zhang, L., Cheng, L., Zhang, X., Cowan, T., Cai, W. & Brutsaert, W. 2015 Groundwater storage trends in the Loess Plateau of China estimated from streamflow records. *Journal of Hydrology* **530**, 281–290.

Gilleland, E. & Roux, G. 2015 A new approach to testing forecast predictive accuracy. *Meteorological Applications* **22** (3), 534–543.

Guangcai, H., Yongping, L., Xiaosi, S., Zhenghong, Z., Zhengping, T., Lihe, Y., Yuncheng, Y. & Xiaoyong, W. 2008 Groundwater systems and resources in the Ordos Basin, China. *Acta Geologica Sinica* **82**, 1061–1069.

Guo, Q., Fu, B., Shi, P., Cudahy, T., Zhang, J. & Xu, H. 2017 Satellite monitoring the spatial-temporal dynamics of desertification in response to climate change and human activities across the Ordos Plateau, China. *Remote Sensing* **9** (6), 525.

Guttman, N. B. 1998 Comparing the palmer drought index and the standardized precipitation index 1. *JAWRA Journal of the American Water Resources Association* **34** (1), 113–121.

Han, Z., Huang, S., Huang, Q., Bai, Q., Leng, G., Wang, H., Zhao, J., Wei, X. & Zheng, X. 2020 Effects of vegetation restoration on groundwater drought in the Loess Plateau, China. *Journal of Hydrology* **591**, 125566.

Han, Z., Huang, S., Huang, Q., Leng, G., Liu, Y., Bai, Q., He, P., Liang, H. & Shi, W. 2021 GRACE-based high-resolution propagation threshold from meteorological to groundwater drought. *Agricultural and Forest Meteorology* **307**, 108476.

Hanasaki, N., Yoshikawa, S., Pokhrel, Y. & Kanae, S. 2018 A global hydrological simulation to specify the sources of water used by humans. *Hydrology & Earth System Sciences* **22** (1), 1–53.

Hargreaves, G. H. & Samani, Z. A. 1985 Reference crop evapotranspiration from temperature. *Applied Engineering in Agriculture* **1** (2), 96–99.

Hayes, M., Svoboda, M., Wall, N. & Widhalm, M. 2011 The Lincoln declaration on drought indices: Universal meteorological drought index recommended. *Bulletin of the American Meteorological Society* **92** (4), 485–488.

Huang, S., Li, P., Huang, Q., Leng, G., Hou, B. & Ma, L. 2017 The propagation from meteorological to hydrological drought and its potential influence factors. *Journal of Hydrology* **547**, 184–195.

Huo, Z., Feng, S., Huang, G., Zheng, Y., Wang, Y. & Guo, P. 2011 Effect of groundwater level depth and irrigation amount on water fluxes at the groundwater table and water use of wheat. *Irrigation and Drainage* **61** (3), 348–356.

Izakian, H., Pedrycz, W. & Jamal, I. 2015 Fuzzy clustering of time series data using dynamic time warping distance. *Engineering Applications of Artificial Intelligence* **39**, 235–244.

Jain, A. K. 2010 Data clustering: 50 years beyond K-means. *Pattern Recognition Letters* **31** (8), 651–666.

Jasechko, S. & Perrone, D. 2021 Global groundwater wells at risk of running dry. *Science* **372** (6540), 418–421.

Jasechko, S., Birks, S. J., Gleeson, T., Wada, Y., Fawcett, P. J., Sharp, Z. D., McDonnell, J. J. & Welker, J. M. 2014 The pronounced seasonality of global groundwater recharge. *Water Resources Research* **50** (11), 8845–8867.

Jiang, X.-W., Wan, L., Wang, X.-S., Wang, D., Wang, H., Wang, J.-Z., Zhang, H., Zhang, Z.-Y. & Zhao, K.-Y. 2018 A multi-method study of regional groundwater circulation in the Ordos Plateau, NW China. *Hydrogeology Journal* **26** (5), 1657–1668.

Ju, Z., Liu, W., Zheng, F. & Liu, J. 2012 Groundwater table dynamics in Qianxian county of Shannxi Province. *Bulletin of Soil and Water Conservation* **32** (2), 178–181.

Kruskal, J. B. & Liberman, M. 1983 The symmetric time-warping problem: From continuous to discrete. In *Time Warps String Edits & Macromolecules the Theory & Practice of Sequence Comparison* (Sankoff, D. & Kruskall, J. B., eds). CSLI Publications, Stanford, CA.

Kubicz, J., Kajewski, I., Kajewska-Szkudlarek, J. & Dąbek, P. B. 2019 Groundwater recharge assessment in dry years. *Environmental Earth Sciences* **78** (18), 555.

Lin, X., Li, W., Bai, X., Han, L. & Ming, D. 2022 Spatial variation in groundwater depletion across China under multiple stresses. *Frontiers in Environmental Science* **10**, 1067766.

Liu, Y., Lei, S., Chen, X., Chen, M., Zhang, X. & Long, L. 2021 Study of plant configuration pattern in guided vegetation restoration: A case study of semiarid underground mining areas in Western China. *Ecological Engineering* **170**, 106334.

Liu, Y., Shan, F., Yue, H., Wang, X. & Fan, Y. 2023 Global analysis of the correlation and propagation among meteorological, agricultural, surface water, and groundwater droughts. *J Environmental Management* **333**, 117460.

Liu, W., Zhang, B., Wei, Z., Wang, Y., Tong, L., Guo, J., Han, X. & Han, C. 2024 Heterogeneity analysis of main driving factors affecting potential evapotranspiration changes across different climate regions. *Science of The Total Environment* **912**, 168991.

Lloyd, S. 1982 Least squares quantization in PCM. *IEEE Transactions on Information Theory* **28** (2), 129–137.

Lloyd-Hughes, B. & Saunders, M. A. 2002 A drought climatology for Europe. *International Journal of Climatology* **22** (13), 1571–1592.

Long, D., Scanlon, B. R., Longuevergne, L., Sun, A. Y., Fernando, D. N. & Save, H. 2013 GRACE satellite monitoring of large depletion in water storage in response to the 2011 drought in Texas. *Geophysical Research Letters* **40** (13), 3395–3401.

Lorenzo-Lacruz, J., Garcia, C. & Morán-Tejeda, E. 2017 Groundwater level responses to precipitation variability in Mediterranean insular aquifers. *Journal of Hydrology* **552**, 516–531.

Lu, C., Zhao, T., Shi, X. & Cao, S. 2018 Ecological restoration by afforestation may increase groundwater depth and create potentially large ecological and water opportunity costs in arid and semiarid China. *Journal of Cleaner Production* **176**, 1213–1222.

Luan, J., Zhang, Y., Li, X., Ma, N., Naeem, S., Xu, Z., He, S., Miao, P., Tian, X. & Wang, R. 2023 Unexpected consequences of large-scale ecological restoration: Groundwater declines are reversed. *Ecological Indicators* **155**, 111008.

Ma, Q., Long, Y., Jia, X., Wang, H. & Li, Y. 2019 Vegetation response to climatic variation and human activities on the Ordos Plateau from 2000 to 2016. *Environmental Earth Sciences* **78** (24), 709.

MacQueen, J. 1967 Some methods for classification and analysis of multivariate observations. *Berkeley Symp. on Math. Statist. and Probability* **5** (1), 281–297.

Mantas, V. M., Liu, Z., Caro, C. & Pereira, A. 2015 Validation of TRMM multi-satellite precipitation analysis (TMPA) products in the Peruvian Andes. *Atmospheric Research* **163**, 132–145.

McKee, T. B., Doesken, N. J. & Kleist, J. 1993 *The Relationship of Drought Frequency and Duration to Time Scales*. California, pp. 179–183.

Meinzer, F. C., Woodruff, D. R., Marias, D. E., Smith, D. D., McCulloh, K. A., Howard, A. R. & Magedman, A. L. 2016 Mapping 'hydroscapes' along the iso- to anisohydric continuum of stomatal regulation of plant water status. *Ecology Letters* **19** (11), 1343–1352.

Mishra, V., Shah, R., Azhar, S., Shah, H., Modi, P. & Kumar, R. 2018 Reconstruction of droughts in India using multiple land-surface models (1951–2015). *Hydrology and Earth System Sciences* **22** (4), 2269–2284.

Noori, R., Maghrebi, M., Jessen, S., Bateni, S. M., Heggy, E., Javadi, S., Noury, M., Pistre, S., Abolfathi, S. & AghaKouchak, A. 2023 Decline in Iran's groundwater recharge. *Nature Communications* **14** (1), 6674.

Ojha, C., Shirzaei, M., Werth, S., Argus, D. F. & Farr, T. G. 2018 Sustained groundwater loss in California's central valley exacerbated by intense drought periods. *Water Resources Research* **54** (7), 4449–4460.

Peters, W., van der Velde, I. R., van Schaik, E., Miller, J. B., Ciais, P., Duarte, H. F., van der Laan-Luijkx, I. T., van der Molen, M. K., Scholze, M., Schaefer, K., Vidale, P. L., Verhoef, A., Wårlind, D., Zhu, D., Tans, P. P., Vaughn, B. & White, J. W. C. 2018 Increased water-use efficiency and reduced CO_2 uptake by plants during droughts at a continental scale. *Nature Geoscience* **11** (10), 744–748.

Petitjean, F., Ketterlin, A. & Gançarski, P. 2011 A global averaging method for dynamic time warping, with applications to clustering. *Pattern Recognition* **44** (3), 678–693.

Qi, S., Feng, Q., Shu, H., Liu, W., Zhu, M., Zhang, C., Yang, L. & Yin, Z. 2023 Redistribution effect of irrigation on shallow groundwater recharge source contributions in an arid agricultural region. *Science of The Total Environment* **865**, 161106.

Scanlon, B. R., Fakhreddine, S., Rateb, A., de Graaf, I., Famiglietti, J., Gleeson, T., Grafton, R. Q., Jobbagy, E., Kebede, S., Kolusu, S. R., Konikow, L. F., Long, D., Mekonnen, M., Schmied, H. M., Mukherjee, A., MacDonald, A., Reedy, R. C., Shamsudduha, M., Simmons, C. T., Sun, A., Taylor, R. G., Villholth, K. G., Vörösmarty, C. J. & Zheng, C. 2023 Global water resources and the role of groundwater in a resilient water future. *Nature Reviews Earth & Environment* **4** (2), 87–101.

Schober, P., Boer, C. & Schwarte, L. A. 2018 Correlation coefficients: Appropriate use and interpretation. *Anesthesia and Analgesia* **126** (5), 1763–1768.

Schreiner-McGraw, A. P. & Ajami, H. 2021 Delayed response of groundwater to multi-year meteorological droughts in the absence of anthropogenic management. *Journal of Hydrology* **603**, 126917.

Schuler, P., Campanyà, J., Moe, H., Doherty, D., Williams, N. H. & McCormack, T. 2022 Mapping the groundwater memory across Ireland: A step towards a groundwater drought susceptibility assessment. *Journal of Hydrology* **612**, 128277.

Shah, D., Shah, H. L., Dave, H. M. & Mishra, V. 2021 Contrasting influence of human activities on agricultural and hydrological droughts in India. *Science of The Total Environment* **774**, 144959.

Shouzhang, P. 2020 1-km monthly precipitation dataset for China (1901-2022). National Tibetan Plateau Data Center.

Sun, Z., Mao, Z., Yang, L., Liu, Z., Han, J., Wanag, H. & He, W. 2021 Impacts of climate change and afforestation on vegetation dynamic in the Mu Us Desert, China. *Ecological Indicators* **129**, 108020.

Teuling, A. J., Van Loon, A. F., Seneviratne, S. I., Lehner, I., Aubinet, M., Heinesch, B., Bernhofer, C., Grünwald, T., Prasse, H. & Spank, U. 2013 Evapotranspiration amplifies European summer drought. *Geophysical Research Letters* **40** (10), 2071–2075.

Thomas, B. F., Famiglietti, J. S., Landerer, F. W., Wiese, D. N., Molotch, N. P. & Argus, D. F. 2017 GRACE groundwater drought index: Evaluation of California central valley groundwater drought. *Remote Sensing of Environment* **198**, 384–392.

Thornthwaite, C. W. 1948 An approach toward a rational classification of climate. *Geographical Review* **38** (1), 55–94.

Tian, W. 2022 *Research on the Impact of Meteorological Drought on Hydrologic Processes and its Regional Regulations*. University of Chinese Academy of Sciences, Beijing.

Tian, H., Cao, C., Chen, W., Bao, S., Yang, B. & Myneni, R. B. 2015 Response of vegetation activity dynamic to climatic change and ecological restoration programs in Inner Mongolia from 2000 to 2012. *Ecological Engineering* **82**, 276–289.

Tijdeman, E., Barker, L. J., Svoboda, M. D. & Stahl, K. 2018 Natural and human influences on the link between meteorological and hydrological drought indices for a large set of catchments in the contiguous United States. *Water Resources Research* **54** (9), 6005–6023.

Udovičić, M., Baždarić, K., Bilić-Zulle, L. & Petrovečki, M. 2007 What we need to know when calculating the coefficient of correlation? *Biochem Med (Zagreb)* **17**, 10–15.

Vicente-Serrano, S. M., Beguería, S. & López-Moreno, J. I. 2010 A multiscalar drought index sensitive to global warming: The standardized precipitation evapotranspiration index. *Journal of Climate* **23** (7), 1696–1718.

Wada, Y., van Beek, L. P. H. & Bierkens, M. F. P. 2012 Nonsustainable groundwater sustaining irrigation: A global assessment. *Water Resources Research* **48** (6), 335–344.

Wada, Y., Wisser, D. & Bierkens, M. F. P. 2014 Global modeling of withdrawal, allocation and consumptive use of surface water and groundwater resources. *Earth System Dynamics* **5** (1), 15–40.

Wan, F., Zhang, F., Wang, Y., Peng, S. & Zheng, X. 2023 Study on the propagation law of meteorological drought to hydrological drought under variable time scale: An example from the Yellow River Water Supply Area in Henan. *Ecological Indicators* **154**, 110873.

Wang, Y., Chen, X., Chen, Y., Liu, M. & Gao, L. 2017 Flood/drought event identification using an effective indicator based on the correlations between multiple time scales of the standardized precipitation index and river discharge. *Theoretical and Applied Climatology* **128** (1), 159–168.

Wendt, D. E., Van Loon, A. F., Scanlon, B. R. & Hannah, D. M. 2021 Managed aquifer recharge as a drought mitigation strategy in heavily-stressed aquifers. *Environmental Research Letters* **16** (1), 014046.

Wu, Y., Liu, T., Paredes, P., Duan, L., Wang, H., Wang, T. & Pereira, L. S. 2016 Ecohydrology of groundwater-dependent grasslands of the semi-arid Horqin sandy land of inner Mongolia focusing on evapotranspiration partition. *Ecohydrology* **9** (6), 1052–1067.

Wu, H., Qian, H., Chen, J. & Huo, C. 2017 Assessment of agricultural drought vulnerability in the Guanzhong Plain, China. *Water Resources Management* **31** (5), 1557–1574.

Xie, X., Xu, C., Wen, Y. & Li, W. 2018 Monitoring groundwater storage changes in the Loess Plateau using GRACE satellite gravity data, hydrological models and coal mining data. *Remote Sensing* **10** (4), 605.

Xie, H.-Y., Jiang, X.-W., Tan, S.-C., Wan, L., Wang, X.-S., Liang, S.-H. & Zeng, Y. 2021 Interaction of soil water and groundwater during the freezing–thawing cycle: Field observations and numerical modeling. *Hydrology and Earth System Sciences* **25** (8), 4243–4257.

Xu, K., Yang, D., Yang, H., Li, Z., Qin, Y. & Shen, Y. 2015 Spatio-temporal variation of drought in China during 1961–2012: A climatic perspective. *Journal of Hydrology* **526**, 253–264.

Yang, X., Zhang, M., He, X., Ren, L., Pan, M., Yu, X., Wei, Z. & Sheffield, J. 2020 Contrasting influences of human activities on hydrological drought regimes over China based on high-resolution simulations. *Water Resources Research* **56** (6), e2019WR025843.

Yao, N., Li, Y., Lei, T. & Peng, L. 2018 Drought evolution, severity and trends in mainland China over 1961–2013. *Science of The Total Environment* **616–617**, 73–89.

Yin, L., Zhang, E., Wang, X., Wenninger, J., Dong, J., Guo, L. & Huang, J. 2012 A GIS-based DRASTIC model for assessing groundwater vulnerability in the Ordos Plateau, China. *Environmental Earth Sciences* **69** (1), 171–185.

Yin, X., Wu, Y., Zhao, W., Zhao, F., Sun, P., Song, Y. & Qiu, L. 2021 Drought characteristics and sensitivity of potential evapotranspiration to climatic factors in the arid and semi-arid areas of northwest China. *Hydrogeology & Engineering Geology* **48** (3), 20–30.

Zhang, Z. & Huisingh, D. 2018 Combating desertification in China: Monitoring, control, management and revegetation. *Journal of Cleaner Production* **182**, 765–775.

Zhang, A. & Jia, G. 2013 Monitoring meteorological drought in semiarid regions using multi-sensor microwave remote sensing data. *Remote Sensing of Environment* **134**, 12–23.

Zhang, M. & Wu, X. 2020 The rebound effects of recent vegetation restoration projects in Mu Us sandy land of China. *Ecological Indicators* **113**, 106228.

Zhang, K., Xie, X., Zhu, B., Meng, S. & Yao, Y. 2019 Unexpected groundwater recovery with decreasing agricultural irrigation in the Yellow River Basin. *Agricultural Water Management* **213**, 858–867.

Zhang, H., Ding, J., Wang, Y., Zhou, D. & Zhu, Q. 2021a Investigation about the correlation and propagation among meteorological, agricultural and groundwater droughts over humid and arid/semi-arid basins in China. *Journal of Hydrology* **603**, 127007.

Zhang, Z., Wang, W., Gong, C., Zhao, M., Franssen, H. H. & Brunner, P. 2021b *Salix psammophila* afforestations can cause a decline of the water table, prevent groundwater recharge and reduce effective infiltration. *Science of The Total Environment* **780**, 146336.

Zhang, H., Zhan, C., Xia, J., Yeh, P. J. F., Ning, L., Hu, S. & Wang, X.-S. 2022a The role of groundwater in the spatio-temporal variations of vegetation water use efficiency in the Ordos Plateau, China. *Journal of Hydrology* **605**, 127332.

Zhang, T., Su, X., Zhang, G., Wu, H., Wang, G. & Chu, J. 2022b Evaluation of the impacts of human activities on propagation from meteorological drought to hydrological drought in the Weihe River Basin, China. *Science of The Total Environment* **819**, 153030.

Zhang, X., Hao, Z., Singh, V. P., Zhang, Y., Feng, S., Xu, Y. & Hao, F. 2022c Drought propagation under global warming: Characteristics, approaches, processes, and controlling factors. *Science of The Total Environment* **838** (Pt 2), 156021.

Zhao, M., Zhang, J., Velicogna, I., Liang, C. & Li, Z. 2020 Ecological restoration impact on total terrestrial water storage. *Nature Sustainability* **4** (1), 56–62.

Zhao, A., Xiang, K., Zhang, A. & Zhang, X. 2022 Spatial-temporal evolution of meteorological and groundwater droughts and their relationship in the North China Plain. *Journal of Hydrology* **610**, 127903.

Zomlot, Z., Verbeiren, B., Huysmans, M. & Batelaan, O. 2015 Spatial distribution of groundwater recharge and base flow: Assessment of controlling factors. *Journal of Hydrology: Regional Studies* **4**, 349–368.

First received 16 April 2024; accepted in revised form 30 July 2024. Available online 28 August 2024